Characterization of Supported Rhodium and Ruthenium Carbonyl Clusters by EXAFS Spectroscopy

Norman Binsted,[†] John Evans,*[†] G. Neville Greaves,[‡] and Richard J. Price[†]

Department of Chemistry, The University, Southampton, S09 5NH, U.K., and SERC Daresbury Laboratory, Warrington, WA4 4AD, U.K.

Received April 26, 1988

Extended X-ray absorption fine structure (EXAFS) spectroscopy has been used to investigate the structure of surface species formed from the interaction of $[Rh_4(CO)_{12}]/\gamma\text{-}Al_2O_3$ and $[Ru_3(CO)_{12}]/SiO_2$. Spherical wave analysis of the spectra was carried out with the inclusion of multiple scattering contributions to third order. This is known to facilitate accurate determination of M–O(CO) distances and assessment of M–C–O bond angles. Rh K-edge EXAFS data on $[Rh_4(CO)_{12}]/\gamma\text{-}Al_2O_3$ established the presence of isolated $Rh(CO)_2$ sites on the oxide surface (Rh–O(surface) = 2.04 Å) after oxidative fragmentation of the initial surface species. Further oxidation resulted in monatomically dispersed Rh centers. The Ru K-edge EXAFS data on the firt chemisorption product of $[Ru_3(CO)_{12}]/SiO_2$ indicates a likely structure of $[Ru_3(CO)_{10}(\mu\text{-}H)(OSi{\equiv})_n]$ ($n = 1$, μ-OSi (bridging), or $n = 2$, OSi≡ (terminal)) (Ru–O(surface) = 2.06 Å), which oxidized in air to give the geminal dicarbonyl species $Ru(CO)_2$ (Ru–O(surface) = 2.08 Å). Vacuum pyrolysis formed hexagonal close-packed metal particles on the surface.

The direct interaction of metal carbonyl clusters with inorganic oxide supports has received considerable attention in terms of catalyst synthesis[1–3] and characterization of adsorbed species.[4–13] In a number of cases decarbonylation is known to occur along with oxidative fragmentation of the cluster. The details of such phenomena are often in doubt, and efforts by this group have involved studying these processes by isotopic substitution and spectral (IR) simulation techniques.[14–16] Diffuse-reflectance measurements of electronic spectra have also been applied to try and identify absorptions due to metal–metal bonding frameworks.

EXAFS measurements can now be made on small metal particles in low concentration for heterogeneous catalysts, hopefully providing a better understanding of catalyst activity and improved catalyst design. X-ray scattering and electron microscopy have been used to give details of particle size and morphology for large particles (<20 Å), but for small particles (<10 Å) structural information has been difficult to obtain. However, the short-range order of EXAFS makes it an ideal structural tool for studying small metal particles and in particular metal clusters supported on inorganic oxides.[16–18] Information on coordination geometries, types of neighboring atoms, interatomic distances, and metal–support interactions becomes available through the technique. A fuller characterization of the surface-supported species is therefore possible and opens up the possibility of understanding catalytic activity with some structural basis.

The interaction of $[Rh_4(CO)_{12}]$ with alumina[8] and $[Ru_3(CO)_{12}]$ with silica[4,6,7] have both been previously reported. Studies have also involved spectral characterization of the fragmentation products by isotope substitution and spectral simulation techniques.[14–16] The reaction schemes for both these systems are given below, along with the ν(CO) IR spectra of the adsorbed species (Figures 1 and 2) isolated at different stages of the oxidative decomposition from the parent cluster.

Scheme I. Reaction Scheme for the Interaction of $[Rh_4(CO)_{12}]$ with Al_2O_3[a]

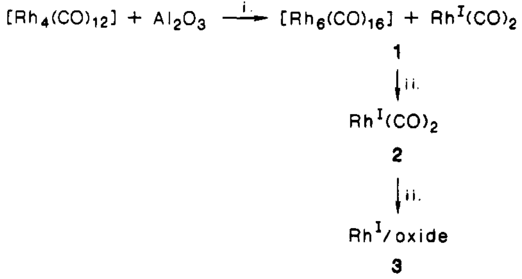

[a] (i) N_2, room temperature; (ii) air.

Scheme II. Reaction Scheme for the Interaction of $[Ru_3(CO)_{12}]$ with SiO_2[a]

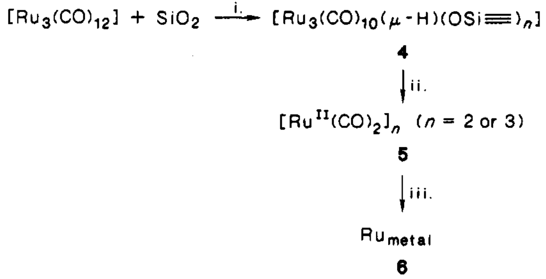

[a] (i) cyclohexane, reflux 70 min; (ii) air, room temperature; (iii) 463 K, 10^{-1} Torr, 15 h.

The initial material 1, which was mauve in color, is a mixture of species. The ν(CO) bands at 2058 and 1803 cm^{-1} have been attributed to $[Rh_6(CO)_{16}]$. Decomposition of 1 takes place on exposure to air, and the transition from 1 to 2 occurs in approximately 4 h. Product 2, with IR ν(CO) bands at 2083 and 2002 cm^{-1}, has been assigned in previous work,[14] as $Rh(CO)_2$ with the metal center having

---

[†] The University.

[‡] SERC Daresbury Laboratory.

(1) Simpson, A. F.; Whyman, R. *J. Organomet. Chem.* **1981**, *213*, 157.

(2) Hunt, D. J.; Jackson, S. D.; Moyes, R. B.; Wells, P. B.; Whyman, R. *J. Chem. Soc., Chem. Commun.* **1982**, 85.

(3) Ferkul, H. E.; Stanton, D. J.; McCowan, J. D.; Baird, M. C. *J. Chem. Soc., Chem. Commun.* **1982**, 955.

(4) Kuznetsov, V. L.; Bell, A. T.; Yermakov, Y. I. *J. Catal.* **1980**, *65*, 374.

(5) Zecchina, A.; Guglielminotti, E.; Bossi, A.; Camia, M. *J. Catal.* **1982**, *74*, 225, 240, 252.

(6) Theolier, A.; Choplin, A.; D'Ornelas, L.; Basset, J. M.; Zanderighi, G.; Ugo, R.; Psaro, R.; Sourisseau, C. *Polyhedron* **1983**, *2*, 119.

(7) Robertson, J.; Webb, G. *Proc. R. Soc. London, Ser. A* **1974**, *341*, 383.

(8) Smith, A. K.; Hugues, F.; Theolier, A.; Basset, J. M.; Ugo, R.; Zanderighi, G. M.; Bilhou, J. L.; Bilhou-Bougnol, V.; Graydon, W. F. *Inorg. Chem.* **1979**, *18*, 3104.

0276-7333/89/2308-0613$01.50/0

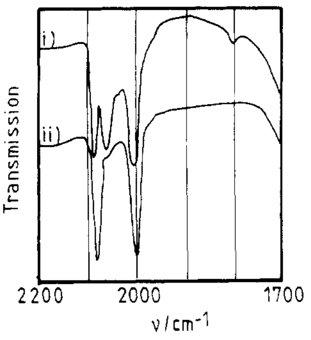

Figure 1. IR spectra for the reaction products of $[Rh_4(CO)_{12}]$ and alumina: (i) after 1 h at room temperature in CH_2Cl_2 under N_2; (ii) sample i after exposure to air for 4 h.

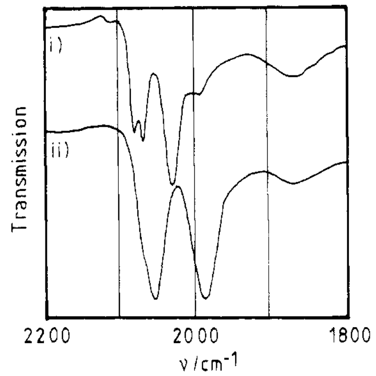

Figure 2. IR spectra for the reaction products of $[Ru_3(CO)_{12}]$ on silica: (i) species **4**; (ii) species **5**. The band at 1880 cm^{-1} is due to the silica support.

an oxidation state of +1. The final product **3**, obtained after extended exposure of **1** to air, showed reversible behavior, with $Rh^I(CO)_2$ being regenerated upon the addition of CO.

The complex nature of the IR spectrum of the orange material **4** with narrow bandwidths is typical of an intact cluster of the type based on a $(X)(Y)M_3(CO)_{10}$ unit (M = Ru, Os).[15-17,19-21] Exposure of **4** to air generated a second orange material (**5**). IR spectra of ^{13}C-enriched samples of **5** and diffuse-reflectance electronic data suggest the likelihood of the surface supported species being $[Ru(CO)_2]_n$ ($n = 2$), with the possibility of a higher oligomer ($n \geq 3$) also being present. The $\nu(CO)$ frequencies indicate a +2 oxidation state for the metal atoms. Vacuum pyrolysis of **5** produced a dark gray material that showed no $\nu(CO)$ stretching bands in the infrared. This is in agreement with work by Basset et al.[22] where thermal decomposition produced metal particles of Ru (14 Å) dispersed on a silica surface. However, the complete decarbonylation of **5** in addition to an inability to regenerate any carbonyl bands upon heating under CO (395 K, 500 Torr, 24 h) was in contrast to previous results obtained by this group using the same conditions.[15]

Experimental Section

General Procedures. $[Ru_3(CO)_{12}]$[23] and $[Rh_4(CO)_{12}]$[24] were prepared by literature methods. γ-Alumina (Aluminoxid C) and silica (Aerosil 380) surfaces (Degussa) were dried at 433 K in vacuo before use. Reaction solvents were dried over CaH_2 and stored over molecular sieves. IR spectra were recorded on a Perkin-Elmer PE580B spectrometer using Nujol mulling agents and NaCl plates. Electronic spectra were recorded on a Perkin-Elmer 554 instrument.

Preparation of Samples 2 and 3 ($[Rh_4(CO)_{12}]/\gamma\text{-}Al_2O_3$). $[Rh_4(CO)_{12}]$ (ca 60 mg) was dissolved in CH_2Cl_2 (ca 120 cm^3) and the solution stirred with the oxide (ca. 700 mg) under a N_2 atmosphere for 1 h. The powder was filtered from the reaction solution and dried in vacuo and the Nujol mull IR spectrum recorded (ν(CO) 2082 (s), 2050 (s), 2001 (s), and 1803 (w) cm^{-1}). Samples of **2** and **3** were obtained by exposing the initial product **1** to air at room temperature for 4 and 12 h, respectively.

Preparation of Samples 4, 5, and 6 ($[Ru_3(CO)_{12}]/SiO_2$). $[Ru_3(CO)_{12}]$ (ca. 80 mg) was dissolved in cyclohexane (ca. 100 cm^3) and the system flushed with N_2 and heated to reflux. Aerosil 380 (ca. 800 mg) was then added and the mixture refluxed with stirring. After 70 min the powder was filtered from the reaction solution, washed with CH_2Cl_2 to remove excess $[Ru_3(CO)_{12}]$, and dried in vacuo (ν(CO) (**4**) 2111 (w), 2076 (s), 2065 (s), 2026 (s), and 1992 (m) cm^{-1}). Sample **5** was obtained by exposing **4** to light and air at room temperature for 3–4 days (ν(CO) (**5**) 2056 (s) and 1992 (s) cm^{-1}). Pyrolysis of **4** to produce **6** was carried out in a glass tube equipped with a greaseless tap and resistive heating coil. After 15 h heating at 430 K under vacuum (0.1 Torr) the surface was completely decarbonylated. Filling the pyrolysis tube with CO (500 Torr) and heating at 395 K for 24 h failed to regenerate any carbonyl species on the surface.

Data Analysis. Ru and Rh K-edge X-ray absorption spectra were recorded on Beam Line 9 on the Synchrotron Radiation Source of the SERC Daresbury Laboratory. Cluster loadings were ca. 1 wt % cluster/surface, and all spectra were recorded in the fluorescence mode using a TlI/NaI scintillation detector.

After background subtraction the spectra were Fourier filtered, using a window broad enough to include all significant structure, in order to remove noise and traces of residual background which might impede refinement. Edge positions were taken as the maximum in the first derivative.

For all calculations the spherical wave theory of Lee and Pendry[25] was used, employing computationally fast algorithms suitable for polycrystalline or amorphous samples.[26,27] Thirteen phase shifts were used in calculating single and double scattering as well as the strong forward scattering term for the triple scattering contribution. However, for the third-order backscattering term only ten phaseshifts were used, this being considered satisfactory for the low atomic numbers and energy ranges in question.[28] Phase shifts for each element were calculated according to the prescription of Loucks[29] by using the muffin-tin approximation to the potentials in the solid.[30] Atomic wave functions were calculated self-consistently by using a relativistic Hartree-Fock program with Slater exchange.[31] No account was

---

(9) Theolier, A.; Smith, A. K.; Leconte, M.; Basset, J. M.; Zanderighi, G. M.; Psaro, R.; Ugo, R. *J. Organomet. Chem.* **1980**, *191*, 415.

(10) Bilhou, J. L.; Bilhou-Bougnol, V.; Graydon, W. F.; Basset, J. M.; Smith, A. K.; Zanderighi, G. M.; Ugo, R. *J. Organomet. Chem.* **1978**, *153*, 73.

(11) Watters, K. L.; Howe, R. F.; Chojnacki, T. P.; Fu, C.-M.; Schneider, K. L.; Wong, N.-B. *J. Catal.* **1980**, *66*, 424.

(12) Knözinger, H.; Thornton, E. W.; Wolf, M. *J. Chem. Soc., Faraday Trans. 1*, **1979**, 1888.

(13) Worley, S. D.; Rice, C. A.; Mattson, G. A.; Curtis, C. W.; Guin, J. A.; Tarrer, A. R. *J. Chem. Phys.* **1982**, *76*, 20.

(14) Evans, J.; McNulty, G. S. *J. Chem. Soc., Dalton Trans.* **1984**, 587.

(15) Evans, J.; McNulty, G. S. *J. Chem. Soc., Dalton Trans.* **1984**, 1123.

(16) Cook, S. L.; Evans, J.; McNulty, G. S.; Greaves, G. N. *J. Chem. Soc., Dalton Trans.* **1986**, 7.

(17) Cook, S. L.; Evans, J.; Greaves, G. N. *J. Chem. Soc., Chem. Commun.* **1983**, 1288.

(18) Binsted, N.; Cook, S. L.; Evans, J.; Greaves, G. N. *J. Chem. Soc., Chem. Commun.* **1985**, 1103.

(19) Besson, B.; Moraweck, B.; Smith, A. K.; Basset, J. M.; Psaro, R.; Fusi, A.; Ugo, R. *J. Chem. Soc., Chem. Commun.* **1980**, 569.

(20) Psaro, R.; Ugo, R.; Zanderighi, G. M.; Besson, B.; Smith, A. K.; Basset, J. M. *J. Organomet. Chem.* **1981**, *213*, 215.

(21) Deeba, M.; Gates, B. C. *J. Catal.* **1981**, *67*, 303.

(22) Basset, J. M.; Choplin, A. *J. Mol. Catal.* **1983**, *21*, 95.

(23) Eady, C. R.; Jackson, P. F.; Johnson, B. F. G.; Lewis, J.; Maltatesta, M. C.; McPartlin, M.; Nelson, W. J. H. *J. Chem. Soc., Dalton Trans.* **1980**, 383.

(24) Chini, P.; Martinengo, S. *Inorg. Chim. Acta* **1969**, *3*, 315.

(25) Lee, P. A.; Pendry, J. B. *Phys. Rev. B* **1975**, *11*, 2795.

(26) Gurman, S. J.; Binsted, N.; Ross, I. *J. Phys. C* **1984**, *17*, 143.

(27) Gurman, S. J.; Binsted, N.; Ross, I. *J. Phys. C* **1986**, *19*, 1845.

(28) Binsted, N.; Cook, S. L.; Evans, J.; Greaves, G. N.; Price, R. J. *J. Am. Chem. Soc.* **1987**, *109*, 3669.

(29) Loucks, T *The Augmented Plane Wave Method*; W. A. Benjamin: New York, 1967.

(30) Mattheis, L. F. *Phys. Rev. A* **1964**, *133*, 1399.

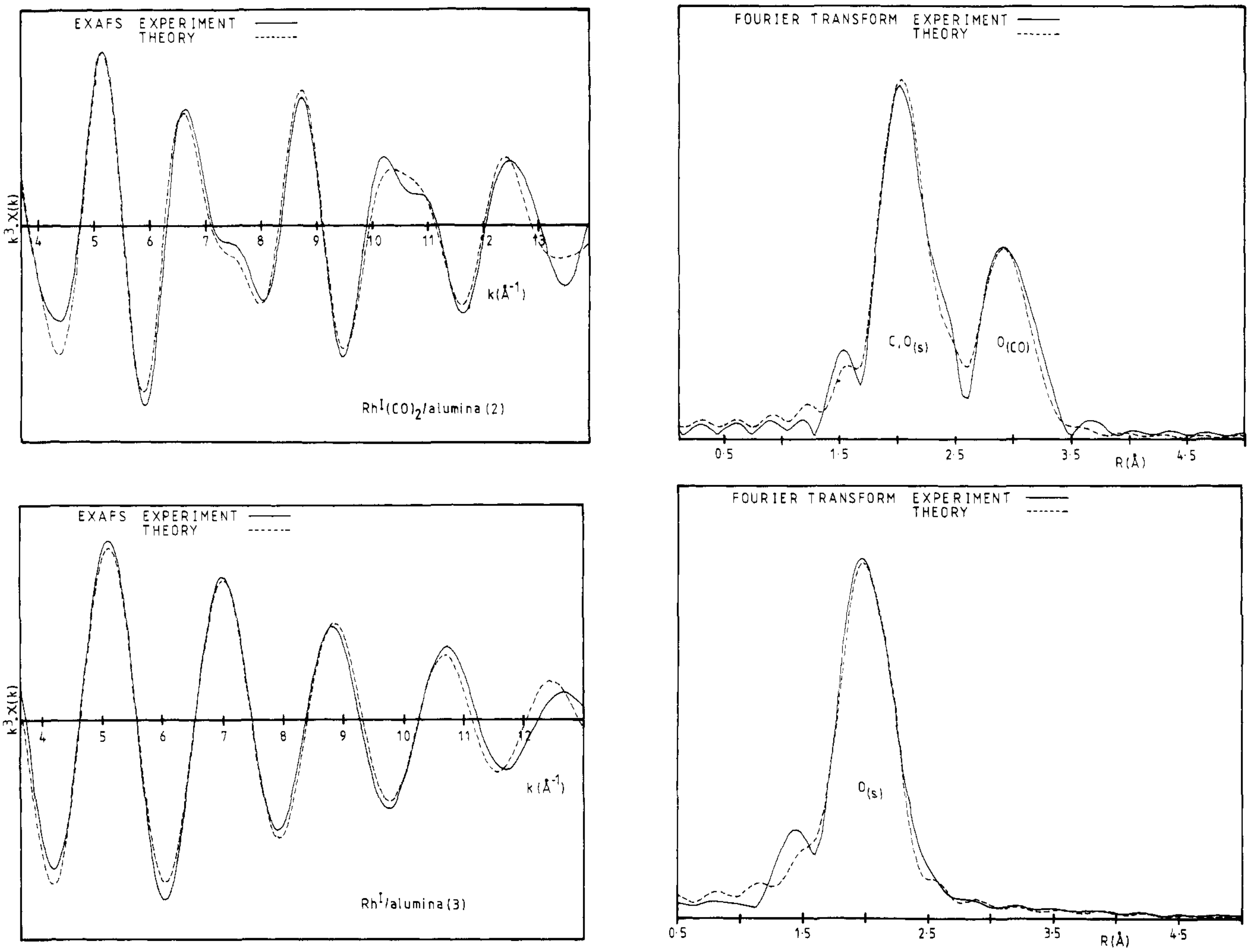

Figure 3. EXAFS and Fourier transforms of the species **2** and **3** isolated from the interaction of $[Rh_4(CO)_{12}]/Al_2O_3$.

taken of the Rh or Ru core holes as prescribed by the final state rule.[32] Previous results indicates that the treatment of the core hole is not critical as over an extreme variation of potential little variation was noted in the interatomic distances determined.[28,33]

The data was analyzed by using k^3-space weighting. A constant imaginary potential of −4 eV was used to model inelastic processes. The reduction in amplitude due to multiple excitations was accounted for by a factor of 0.62. This was the refined value obtained when fitting the Rh K-edge EXAFS of rhodium metal. Interatomic distances, Debye–Waller factors, E_0 (the energy origin of the photoelectron), selected occupation numbers, and M–C–O bond angles were all refined.

IR spectra were recorded for all the samples, before and after the EXAFS spectra were run, to check for radiation damage. All surface species were found to have consistent ν(CO) stretching bands.

The importance of using spherical wave-multiple scattering calculations has previously been assessed in the analysis of cobalt carbonyl complexes.[28] The inclusion of scattering terms up to third order was found to be adequate in describing the spectra to within a few electronvolts of the absorption edge and determination of interatomic distances to within 0.03 Å. The angular dependence of multiple scattering within a M–C–O unit also allows the possibility of accurate bond angle determination and this has been used with some success for a number of unsupported transition metal carbonyls.[28,34] The guidelines established in previous work form the basis for the analysis of our spectra of supported transition-metal complexes. Results are reported (Table I) in terms of the discrepancy index

$$R = \int |\chi^T(k) - \chi^E(k)|k^3\,dk \Big/ \int |\chi^E(k)|k^3 dk \times 100\%$$

and the Fit index

$$FI = \sum_i ((k_i)^n(\chi_i^T - \chi_i^E))^2$$

Results

$Rh^I(CO)_2/\gamma\text{-}Al_2O_3$ (2). The Fourier transform of the EXAFS spectrum (Figure 3) indicates the presence of two main backscattering shells. The first shell was found to contain information from two different interactions: Rh–C (1.81 Å) and Rh–O(surface) (2.04 Å). The second shell was satisfactorily fitted by using a single Rh–O(CO) distance of 3.00 Å. The EXAFS derived data are therefore consistent with a rhodium dicarbonyl unit attached to the alumina surface via Rh–O bonds. The occupation number for this metal–oxide interaction refined to the exceptionally high value of N(Rh–O(surface)) = 7.0 (2). A structurally analogous $Rh^I(CO)_2$ species on alumina studied by van't Blik et al.[35-37] has been reported to have rhodium atoms coordinated to approximately three surface oxygen atoms with a longer Rh–O(surface) distance of 2.12 Å.

---

(31) Program by J. P. Desclaux, modified by P. J. Durham.

(32) von Barth, U.; Grossman, G. *Phys. Rev. B* **1982**, *25*, 5150.

(33) Price, R. J. Ph.D Thesis, Southampton University, 1987.

(34) Binsted, N.; Evans, J.; Greaves, G. N.; Price, R. J. *J. Chem. Soc., Chem. Commun.* **1987**, 1330.

(35) van't Blik, H. F. J.; van Zon, J. B. A. D.; Huizinga, T.; Vis, J. C.; Koningsberger, D. C.; Prins, R. *J. Phys. Chem.* **1983**, *87*, 2264.

(36) van't Blik, H. F. J.; van Zon, J. B. A. D.; Huizinga, T.; Vis, J. C.; Koningsberger, D. C.; Prins, R. *J. Phys. Chem.* **1985**, *107*, 3139.

(37) van Zon, J. B. A. D.; Koningsberger, D. C.; van't Blik, H. F. J.; Sayers, D. E. *J. Chem. Phys.* **1985**, *82*, 5742.

Table I. Ru and Rh K-Edge EXAFS Derived Data: Interatomic Distances (R), Debye–Waller Factors ($A = 2\sigma^2$), Occupation Numbers (N), and Bond Angles (M–C–O)[a]

compound	backscattering shell	N^b	R, Å	A, Å^2	M–C–O, deg	E_0, eV	R, %	FI
$Rh(CO)_2/Al_2O_3$ (2)	Rh–C	2.0	1.814 (2)	0.0046 (4)	164 (2)	24.9 (4)	17.0	0.26
	Rh–O(s)	7.0 (2)	2.038 (2)	0.0209 (9)				
	Rh–O(CO)	2.0	3.003 (3)	0.0103 (12)				
Rh/Al_2O_3 (3)	Rh–O(s)	6.0 (1)	2.033 (1)	0.0109 (4)		24.7 (2)	c	0.36
$[Ru_3(CO)_{10}(\mu\text{-}H)(OSi{\equiv})_n]$ (4)	Ru–C	3.3	1.895 (2)	0.0046 (4)	165 (1)	27.5 (3)	16.2	0.53
	Ru–O(s)	3.8 (4)	2.056 (4)	0.0227 (32)				
	Ru–Ru	2.0	2.792 (2)	0.0121 (5)				
	Ru–O(CO)	3.3	3.064 (2)	0.0035 (8)				
$Ru(CO)_2/SiO_2$ (5)	Ru–C	2.0	1.870 (3)	0.0030 (6)	163 (1)	27.3 (4)	18.1	0.37
	Ru–O(s)	4.9 (2)	2.079 (2)	0.0119 (11)				
	Ru–O(CO)	2.0	3.011 (3)	0.0037 (8)				
Ru_{metal}/SiO_2 (6)	Ru–Ru	12.0	2.673 (2)	0.0118 (2)		25.0 (5)	c	2.54
	Ru–Ru	6.0	3.762 (7)	0.0163 (13)				
	Ru–Ru	2.0	4.397 (12)	0.0081 (20)				
	Ru–Ru	18.0	4.630 (6)	0.0181 (13)				
	Ru–Ru	12.0	5.130 (14)	0.0183 (25)				
	Ru–Ru	6.0	5.272 (5)	0.0056 (7)				

[a] Standard deviations in parentheses. Quoted values are those obtained from the least-squares analyses, with no allowance for parameter correlation. Likely errors for bonded and nonbonded distances (including systematic errors) have been estimated as 1.4 and 1.6%. Corker, J. M.; Evans, J.; Leach, H.; Levason, W. *J. Chem. Soc., Chem. Commun.*, in press. Values without standard deviations were held fixed. R, % = discrepancy index. FI = fit index. E_0 = energy origin of photoelectron. s = surface. [b] Values held constant were for the coordination numbers of the structures derived from IR experiments for the carbonyl centers.[14,15] Bulk metal values were used for the Ru/SiO_2 sample, the spectrum being very similar to that of the metal foil. [c] Data not available for single scattering fitting routines at the time of analysis.

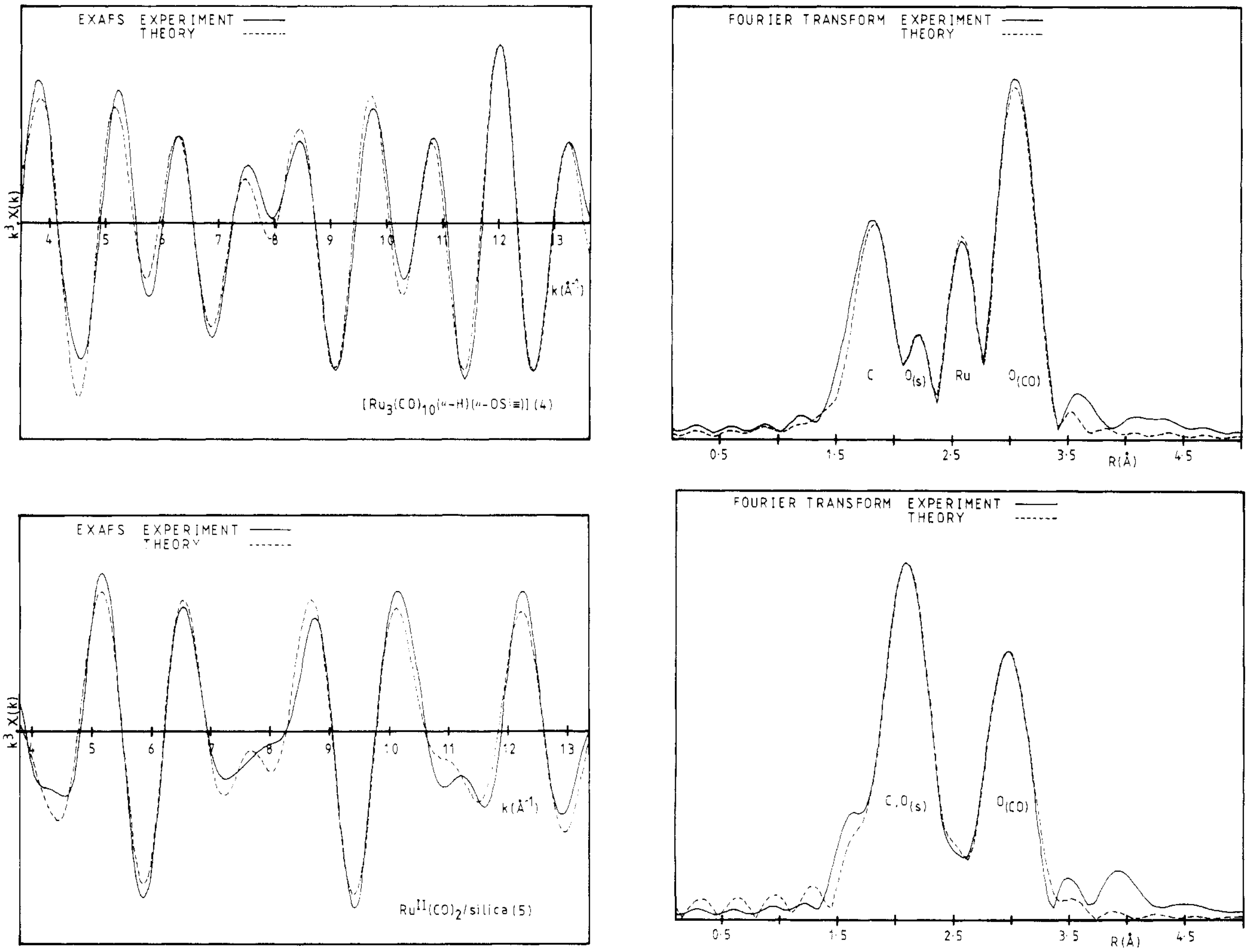

Figure 4. EXAFS and Fourier transforms of the species **4** and **5** isolated from the interaction of $[Ru_3(CO)_{12}]/SiO_2$.

$Rh^I/\gamma\text{-}Al_2O_3$ (3). The spectrum of **3** (Figure 3) reveals one strong backscattering shell with an amplitude envelope typical for that of a light element. The data was fitted by using a Rh–O(surface) interaction of 2.03 Å. This distance is comparable to that observed between the rhodium centers and the alumina surface in **2**, suggesting a comparable average oxidation state for the metal.

The occupation number for the Rh-oxide interaction refined to the high value of 6.0 (1), suggesting the possibility that the metal atoms were diffused into the defect

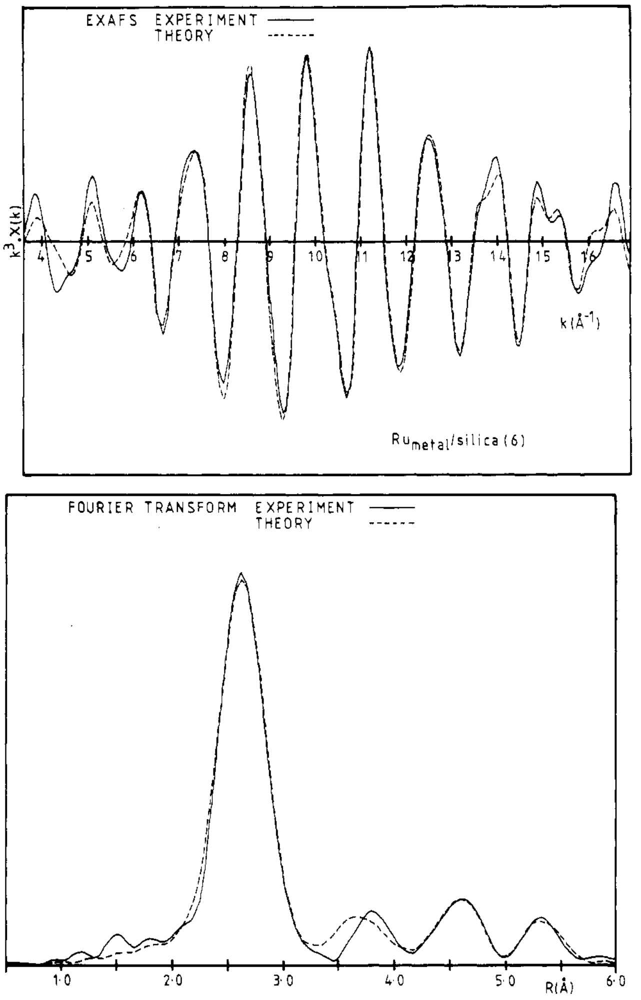

Figure 5. EXAFS and Fourier transforms of the species **6** isolated from the interaction of $[Ru_3(CO)_{12}]/SiO_2$.

spinel structure of the γ-Al_2O_3. Although this behavior has been observed in other systems,[38-40] it is unlikely in this instance as stronger contributions from minor scattering shells (not present in the Fourier filtered data) would be expected.[38,39] The minor backscattering shells present in the unfiltered data were too weak to be fitted in the analysis; however, their amplitude envelope was indicative of a heavy backscattering element. This is most likely due to the presence of other rhodium atoms on the surface, but the occupation numbers are so low that **3** can effectively be considered to consist of atomically dispersed rhodium. The ease with which species **2** can be regenerated from **3** supports these conclusions.

The occupation number N(Rh–O(surface)) = 6.0 (1) was also considered to be possible indicative of a hexaaquorhodium(III) species[41] being formed on the surface. However, electronic spectroscopic data failed to provide any evidence for such a species.

$[Ru_3(CO)_{10}(\mu\text{-}H)(OSi{\equiv})_n]$ (n = 1 or 2) (4). The chemisorption of $[Ru_3(CO)_{12}]$ on silica and $[Os_3(CO)_{12}]$ on alumina is now generally agreed to afford similar types of species as the first observable product based on a (X)(Y)$M_3(CO)_{10}$ unit.[15-17,19-21] It has, however, proved difficult to differentiate between the three alternative structures shown in Figure 6. Recently vibrational spectroscopic evidence for the presence of bridging hydride sites on the oxide surface has recently been reported,[42] indicating that the species formed is either of type **4i** or **4iii**.

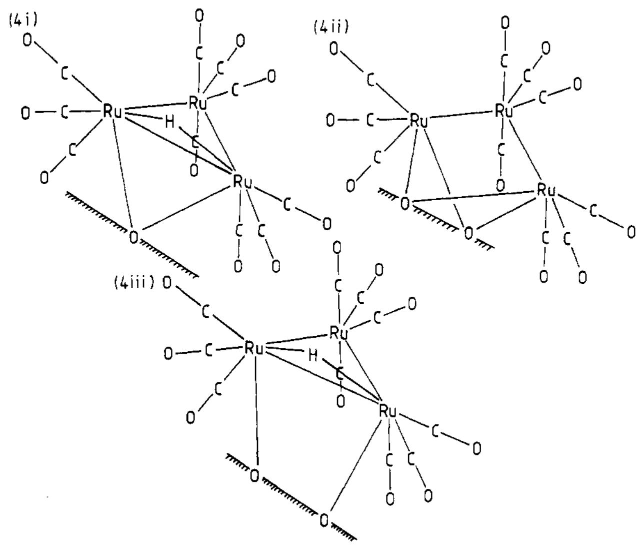

Figure 6. Possible structures for the first chemisorption product of $[Ru_3(CO)_{12}]$ on silica.

The analysis of the EXAFS of the ruthenium species provides additional structural information. The Fourier transform (Figure 4) shows four distinct backscattering environments. These were fitted with Ru–C, Ru–O(surface), Ru–Ru, and Ru–O(CO) interactions at increasing interatomic distances. Only one Ru–Ru distance was refinable, consistent with crystallographic data on osmium-containing models of structure types **4i** and **4iii**[43] but inconsistent with type **4ii**.[44] The determination of occupation numbers for the metal–oxide interactions appears to be unrealistically high for all the surface species studied in this work (Table I). This makes assessment of the type and number of ligands with which cluster **4** is attached to the surface difficult. Distinguishing whether one bridging (**4i**) or two terminal (**4iii**) oxygen atoms of the support are involved anyway is not possible from the EXAFS analysis since each affords the same mean coordination number for Ru. All the bond distances derived for the species are within 0.03 Å of those observed in model osmium species of structure types **4i** and **4iii**; the similarity of the covalent radii of ruthenium and osmium would suggest that they are chemically reasonable values. In addition, the most recent EXAFS analysis of Os L(III) edge data on the $[Os_3(CO)_{12}]/Al_2O_3$ species[45] is also consistent with either of structure types **4i** and **4iii**.

The Raman spectrum of such a sample[46] in the Os–Os stretching region matches with those of model complexes of **4iii** more closely than with models of **4i**.[42] Recently, ^{13}C CP-MAS NMR evidence has been presented for the analogous $[Os_3(CO)_{12}]/SiO_2$ system which was interpreted as favoring structure **4i**.[47] This involved a comparative extrapolation from the ^{13}CO chemical shifts of two model compounds, $[HOs_3(CO)_{10}(OSiEt_3)]$ and $[HOs_3(CO)_{10}(O_2C$-

---

[38] Greegor, R. B.; Lytle, F. W.; Chin, R. L.; Hercules, D. M. *J. Phys. Chem.* **1981**, *85*, 1232.

[39] Friedman, R. M.; Freeman, J. L.; Lytle, F. W. *J. Catal.* **1978**, *55*, 10.

[40] Yao, H. C.; Japar, S.; Shelef, M. J. *J. Catal.* **1977**, *50*, 407.

[41] Jørgensen, C. K. *Acta Chem. Scand.* **1956**, *10*, 500.

[42] Alexiev, V. D.; Binsted, N.; Evans, J.; Greaves, G. N.; Price, R. J. *J. Chem. Soc., Chem. Commun.* **1987**, 395.

[43] Churchill, M. R.; Wasserman, H. J. *Inorg. Chem.* **1980**, *19*, 2391.

[44] Allen, V. F.; Mason, R.; Hitchcock, P. B. *J. Organomet. Chem.* **1977**, *16*, 2697.

[45] Duivenvoorden, F. B. M.; Koningsberger, D. C.; Uh, Y. S.; Gates, B. C. *J. Am. Chem. Soc.* **1986**, *108*, 6254.

[46] Deeba, M.; Steusand, B. J.; Schrader, G. L.; Gates, B. C. *J. Catal.* **1981**, *69*, 218.

[47] Walter, T. H.; Frauenhoff, G. R.; Shapley, J. R.; Oldfield, E. *Inorg. Chem.* **1988**, *27*, 2561.

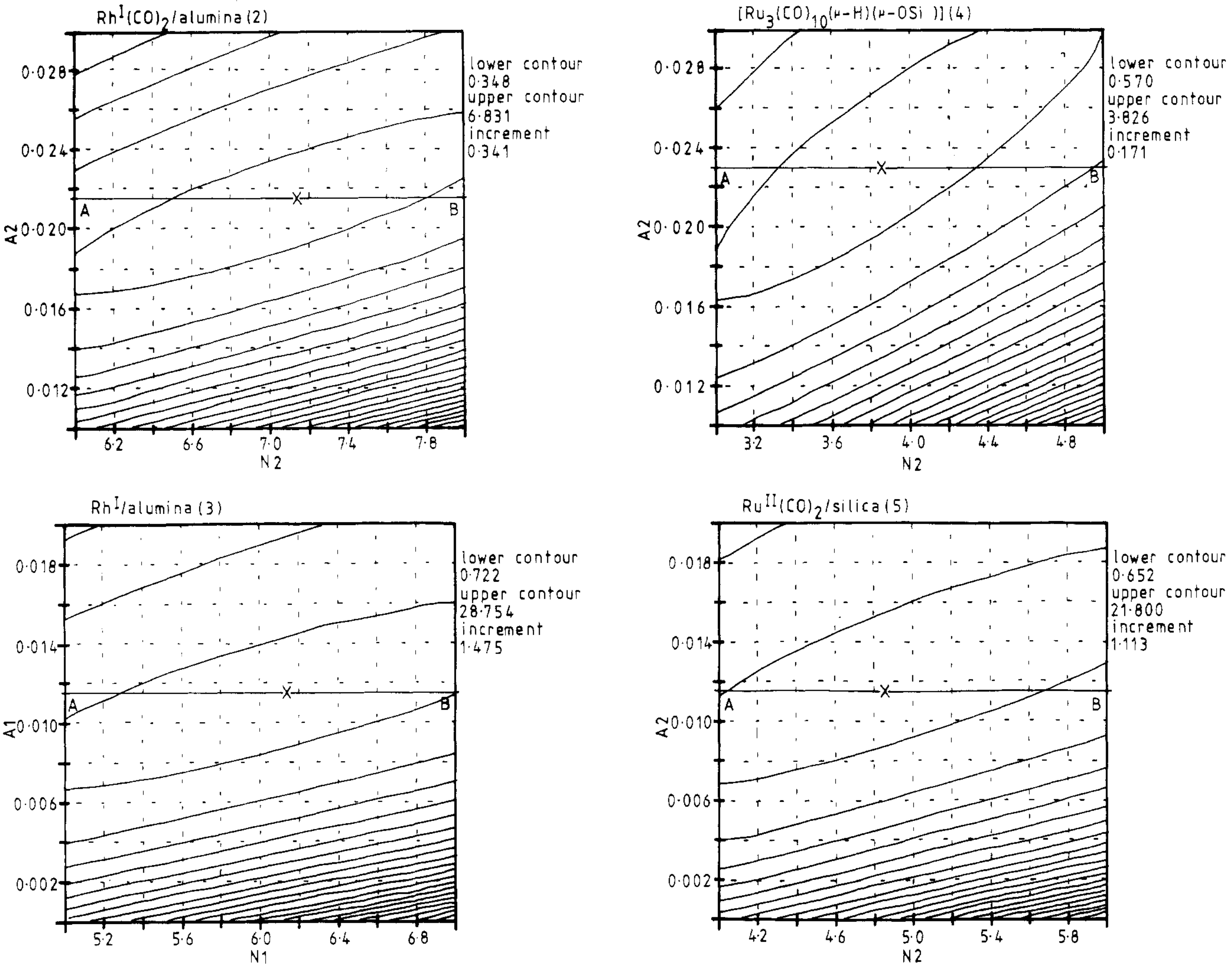

Figure 7. Fit index contour maps for the correlations between N(M–O(surface)) and associated Debye–Waller factors.

H)], to the values observed on the silica surface species and is also subject to uncertainty. It may be that different surface sites are adopted on silica and alumina. Some supporting evidence for the utilisation of an isolated silanol group in the oxidative addition reaction to form **4** is provided by the observation of their preferential reactivity with supported rhodium during the CO-induced oxidation to Rh^1 centers.[48] This offers a route to the formation of a bridging siloxide ligand as in **4i**.

$Ru^{II}(CO)_2/SiO_2$ (5). The Fourier transform of the EXAFS spectrum of **5** (Figure 4) with two main backscattering shells is very similar to that of **2**. The data was fitted with a three shell model in accordance with ruthenium dicarbonyl units attached to the surface via Ru–O bonds. Previous work carried out on the characterization of **5** identified the species as an oligomer of a $Ru(CO)_2$ moiety; dimeric $[Ru_2(CO)_4]$ and cyclic $[Ru_3(CO)_6]$ models were both proposed.[13] However, the EXAFS data in this instance provide no evidence for any strong metal–metal interactions. This discrepancy is likely to be related to sample age and pretreatment of the silica surface.

Ru_{metal}/SiO_2 (6). The EXAFS spectrum of **6** (Figure 5) shows an almost identical fine structure and Fourier transform to that of bulk ruthenium metal. The first six backscattering shells were Fourier filtered and fitted with a hexagonal close-packed structure. Fits were also produced assuming face-centered cubic and body-centered cubic arrangements of the metal atoms, yielding the following series of fit indices: FI(hcp) = 2.54; FI(fcc) = 3.46; FI(bcc) = 5.19. This range of FI's is such as to indicate that the metal atoms are indeed hexagonally close packed. No evidence for the interaction between interfacial metal atoms and the surface oxygen atom was observed, indicating a relatively large size of metal particle. Electron microscopy studies on Ru/SiO_2[49] have revealed two types of supported metal clusters; a two-dimensional raftlike structure with a diameter between 40 and 60 Å and a larger three-dimensional particle with diameters greater than 60 Å. The EXAFS data for species **6** is consistent with the latter type of particles and a hexagonal close-packed arrangement of the metal atoms. The particles are large enough to be resistant to attack by CO at 395 K.

Determination of the Metal–Oxide Occupation Numbers N(M–O(surface)). The determination of the occupation numbers for the metal–oxide interaction all refine to values that appear unrealistically high. Coordination numbers for the two ruthenium species **4** and **5** are lower than those for the rhodium species **2** and **3**; a reflection of the more open structure of the silica surface[50] in comparison to that of alumina.[51] Associated with these high coordination numbers are large Debye–Waller factors,

---

[48] Basu, P.; Panayotov, D.; Yates, J. T., Jr. *J. Phys. Chem.* **1987**, *91*, 3133.

[49] Prestridge, E. B.; Via, G. H.; Sinfelt, J. H. *J. Catal.* **1977**, *50*, 115.

[50] Peri, J. B.; Hensley, S. L. *J. Phys. Chem.* **1968**, *72*, 2926.

[51] Peri, J. B. *J. Phys. Chem.* **1965**, *69*, 211, 220.

indicating a large amount of disorder within these particular shells.

The theory used in our analysis procedures assumes a Gaussian distribution of distances in any shell when determining the Debye–Waller factor. Although no real pair distribution function is purely Gaussian many systems with a small degree of disorder can be fairly accurately described as such. Asymmetric pair correlation functions and anharmonic vibration potentials can introduce large static and thermal disorders.[52] Failure to take these factors into account can lead to serious errors through modification in the EXAFS amplitude and apparent change in the nearest-neighbor distance. Much of the important information on the pair distribution function is contained in the low-energy region of an EXAFS spectrum ($k < 3$ Å^{-1})[53] where the simple backscattering picture does not apply. The low-energy cut is usually taken around $k_{\min} = 3$ Å^{-1} by virtue of edge complications. This can therefore frustrate attempts to deal with the problem of large disorders.

The Debye–Waller factors obtained for species **2**, **3**, **4**, and **5** (0.011–0.023 Å^2) are indicative of large disorders, and it is felt that this lies at the heart of the problem of unrealistic occupation number determination for N(M–O(surface)). A number of different interactions are likely to exist between the metal atoms and the oxide surface, resulting in a large static and/or thermal disorders. Studying the supported species at liquid N_2 temperatures would reduce the disorder from thermal vibrations and may allow more accurate determination of the occupation numbers, but the static disorder, likely to be a very significant component, would still persist.

In addition to these problems, it is known that one of the drawbacks with multishell fitting techniques is that high correlations can develop between some parameters. This is evident in the four Fit index contour maps (Figure 7) for the correlations between the M–O(surface) occupation numbers and the associated Debye–Waller factors. The maps are produced by allowing each parameter to vary over a defined range and plotting contours of the Fit index. The elliptical shape of the contours on each map bears testimony to the strength of the correlations involved and the resulting poor definition in the determined occupation numbers. It has been suggested recently that a more accurate estimate of the standard deviations may be obtained by using the ratio of the principal axis length of the ellipse to that of a horizontal section through the contours.[54] Clearly in all these cases the error will be at least ±1 in the coordination number.

Bond Angle Determination. The use of multiple-scattering theory in the analysis of EXAFS data allows for accurate determination of M–O(CO) distances in transition-metal carbonyl clusters. In addition, there is a potential for calculating M–C–O bond angles in carbonyl ligands.[28,34,42] Species **2**, **4**, and **5** were all determined to have been carbonyl ligands (M–C–O = 163–165°). However, IR ν(CO) evidence for the species indicates the presence of straight terminal carbonyl ligands. In species **2** and **5** the ligands are directed away from the oxide surface and it would indeed seem unlikely that the ligands are bent. In the case of **4** it is conceivable that some of the ligands are distorted to alleviate interactions between the cluster and the silica surface. However, the low cluster loading on the surface (<1 wt %) means that the cluster interacts with approximately one in every 250 surface hydroxyl groups present (assuming 5 OH/nm^2 of surface). The cluster may therefore be positioned on atypical sites, thereby avoiding any strong interactions between the carbonyl ligands and the oxide surface. Attempts were made to introduce M–M, M–Al, and M–Si interactions into the models fitted for **2** and **5**. Unreasonable Debye–Waller factors and/or distances were obtained for the additional shells, and no straightening of the M–C–O bond angles was observed. Interestingly, Hoffman et al.[55] have made a qualitative study of alternative coordination models of diatomic ligands in transition-metal complexes. They suggest a strategy for bending the usually linear M–C–O unit, but as yet no examples of mononuclear complexes with bent carbonyl ligands exist (excluding deviations of <15° attributed to crystal packing distortions). The estimation of the M–C–O bond angles for **2**, **4**, and **5** would therefore appear to be systematically low. This is disappointing in light of the success achieved in the determination of bond angles in unsupported transition-metal carbonyl clusters. This may be due to the presence of some non-carbonyl species on the oxide surface. Then the real coordination number would be lower than that used in these curve-fitting procedures. Overestimating the coordination number would have the effect of lowering the bond angle.[28]

Chart I. Summary of the Structural Models and Parameters Used in Fitting the EXAFS Spectra of the Supported Species Obtained from the Interaction of $[Rh_4(CO)_{12}]/Al_2O_3$ and $[Ru_3(CO)_{12}]/SiO_2$

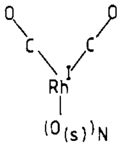

Rh–C = 1.81 Å
Rh–O(surface) = 2.04 Å
Rh–O(CO) = 3.00 Å
N(Rh–O(surface)) = 7.0
∠Rh–C–O = 164°

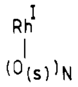

Rh–O(surface) = 2.03 Å
N(Rh–O(surface)) = 6.0

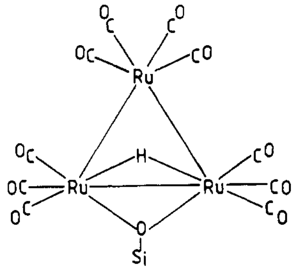

Ru–C = 1.90 Å
Ru–O(surface) = 2.06 Å
Ru–Ru = 2.79 Å
Ru–O(CO) = 3.06 Å
N(Ru–O(surface)) = 3.8
∠Ru–C–O = 165°

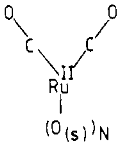

Ru–C = 1.87 Å
Ru–O(surface) = 2.08 Å
Ru–O(CO) = 3.01 Å
N(Ru–O(surface)) = 4.9
∠Ru–C–O = 163°

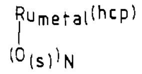

Ru–Ru = 2.68 Å (nearest neighbor)

In principle one may refine the bond angle, coordination number, and Debye–Waller factors. But these parameters are all strongly correlated and attempting to refine the third intensity-related parameter is likely to render all three indeterminate. Assessing coordination numbers, particularly for nonbonded shells which contribute a minor proportion of the total back-scattering, remains a difficult

---

[52] Teo, B. K. *EXAFS: Basic Principles and Data Analysis*; Springer-Verlag: New York, 1986.

[53] Eisenberger, P.; Brown, G. S. *Solid State Commun.* **1979**, *29*, 481.

[54] Joyner, R. W.; Martin, K. J.; Meehan, P. *J. Phys. C* **1987**, *20*, 4005.

[55] Hoffman, R.; Chen, M. M.-L.; Thorn, D. L. *Inorg. Chem.* **1977**, *16*, 503.

area for EXAFS. Many "real" problems provide experimental difficulties in gaining the long (>1 keV) data ranges with good signal-to-noise ratio necessary for such assessments.

A summary of the structural models and parameters used in fitting the EXAFS spectra of the supported species is shown in Chart I. Determination of interatomic distances, coordination numbers, and bond angles allows for a more detailed structural analysis of **2**, **3**, **4**, **5**, and **6** than has previously been obtained. Information on the M–O(surface) interaction is of particular interest as it is believed to play an important role in determining catalytic activity and selectivity for ultra-dispersed supported metals.

Distance determinations from the EXAFS data are reliable and accurate in contrast to the determination of occupation numbers. The values of N(M–O(surface)) obtained for **2**, **3**, **4**, and **5** would appear to be unrealistically high. It is felt that this is a result of large (probably) static disorders and high correlations between parameters. The nonideal nature of the interaction between mononuclear metal complexes or small metal clusters attached to the bulk of an oxide surface would therefore appear to present problems for accurate occupation number determination.

The incongruity between the IR data and determination of M–C–O bond angles by EXAFS suggests that a systematic error is involved in the determination of this parameter, which may also be due to the treatment of disorder as due to a single, isotropic factor.

Acknowledgment. We wish to thank SERC for a research studentship (R.J.P.), a research assistantship (N.B.), and use of the Daresbury Laboratory facilities. We also thank Johnson Matthey and Degussa for the ruthenium chloride and oxide samples, respectively.

Registry No. $Rh(CO)_{12}$, 19584-30-6; $Ru(CO)_{12}$, 15243-33-1; Al_2O_3, 1344-28-1; SiO_2, 7631-86-9.

Spectroscopic and Electrochemical Study of Trinuclear Ferracyclopentadienyl Clusters $[Fe_3(\mu\text{-}CO)_2(CO)_6(RC_2R)_2]$

Domenico Osella,* Giuseppina Arman, Mauro Botta, and Roberto Gobetto

Dipartimento di Chimica Inorganica, Chimica Fisica e Chimica dei Materiali, Università di Torino, Via Pietro Giuria 7, 10125 Torino, Italy

Franco Laschi and Piero Zanello*

Dipartimento di Chimica, Università di Siena, 53100 Siena, Italy

Received May 6, 1988

The redox chemistry of triiron metallacyclopentadienyl clusters $Fe_3(CO)_8(RC_2R)_2$ has been investigated by electrochemical and spectroscopic techniques. Their ^1H and ^{13}CNMR resonances have been assigned by comparison of the NMR data of different isomers and by two-dimensional and selective decoupling experiments. The sequence of electrode processes has been postulated on the basis of the response of cyclic voltammetry (CV), coulometry, electron spin resonance (ESR) spectroscopy, and chemical tests. The influence of the metallacyclopentadienyl ring substituents on the trend of the redox potentials supports the high electronic delocalization in the Fe_3C_4 skeleton previously postulated on the basis of theoretical calculations. Finally, an effective electron transfer catalyzed (ETC) synthesis of the two $[Fe_3(CO)_7P(OMe)_3(PhC_2Ph)_2]$ isomers has been achieved.

Introduction

Acetylene metal cluster compounds show a variety of structural arrangements that are suitable models for chemisorbed hydrocarbons on metallic surfaces.[1] It was recognized some time ago that the major products in the reactions between iron carbonyls and alkynes are complexes of the type $Fe_3(CO)_8(alkyne)_2$.[2,3] Such systems, which contain a ferracyclopentadienyl ring, are quite common in organometallic chemistry and have been considered as intermediates in the cyclotrimerization of alkynes.[4]

An X-ray structure study of $Fe_3(CO)_8(PhC_2Ph)_2$ (**1**) has been reported by Dodge et al.:[5] the metallic framework consists of an open triangle whose two edges are asymmetrically bridged by CO's and in which the metallacycle plane intersects the Fe_3 plane perpendicularly; the phenyl groups are twisted away from the FeC_4 plane in the same sense, all by about 55°. Two ^{13}C NMR studies have shown that this structural arrangement is maintained in solution and that CO ligands exchange locally on each Fe′ atom.[6,7] The electronic structure of molecules containing a pentaatomic metallacycle has received considerable attention since Hoffmann et al.[8] suggested that polynuclear metallacyclopentadienyl compounds are suitable candidates to exhibit a six-π-electron aromaticity. Combined UV-PES

---

[1] (a) Ugo, R. *Catal. Rev.* **1975**, *11*, 225. (b) Muetterties, E. L.; Rhodin, T. N.; Bond, E.; Brucker, C. F.; Pretzer, W. R. *Chem. Rev.* **1979**, *79*, 91.

[2] Hubel, W. In *Organic Syntheses via Metal Carbonyls*; Wender, I., Pino, P., Eds.; Wiley-Interscience: New York, 1968.

[3] Fehlhammer, W. R.; Stolzenberg, H. In *Comprehensive Organometallic Chemistry*; Wilkinson, G., Stone, F. G. A., Abel, E. W., Eds.; Pergamon: Oxford, 1982.

[4] Vollhardt, K. P. C. *Acc. Chem. Res.* **1977**, *10*, 1.

[5] Dodge, R. P.; Schomaker, V. *J. Organomet. Chem.* **1965**, *3*, 274.

[6] Hickey, J. P.; Wilkinson, J. R.; Todd, L. J. *J. Organomet. Chem.* **1975**, *99*, 281.

[7] Aime, S.; Milone, L.; Sappa, E. *Inorg. Chim. Acta* **1976**, *16*, L7.

[8] Thorn, D. L.; Hoffmann, R. *Nouv. J. Chim.* **1979**, *3*, 39.

0276-7333/89/2308-0620$01.50/0 © 1989 American Chemical Society